Gerda

Progress report to the LNGS scientific committee
(Appendix)
LNGS-EXP 33/05 add. 11/10
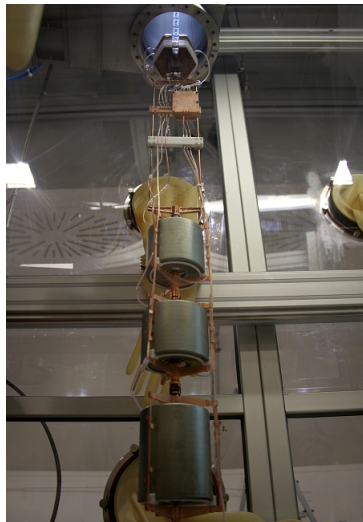
This Gerda report summarizes the progress achieved during the last six months. A *Short Write-up* is linked at:

http://www.mpi-hd.mpg.de/GERDA/reportsLNGS/gerda-lngs-sc-oct10-shwup.pdf.

Experimental and technical details are given in the *Appendix* which is linked at:

http://www.mpi-hd.mpg.de/GERDA/reportsLNGS/gerda-lngs-sc-oct10-appdx.pdf.

Previous reports are available at: http://www.mpi-hd.mpg.de/GERDA/reportsLNGS.

October 2010

H. Aghaei[m], M. Agostini[f], M. Allardt[c], A.M. Bakalyarov[l], M. Balata[a], I. Barabanov[j], M. Barnabe-Heider[f], L. Baudis[r], C. Bauer[f], N. Becerici-Schmid[m], E. Bellotti[g,h], S. Belogurov[k,j], S.T. Belyaev[l], A. Bettini[n,o], L. Bezrukov[j], T. Bruch[r], V. Brudanin[d], R. Brugnera[n,o], D. Budjas[f], A. Caldwell[m], C. Cattadori[g,h], F. Cossavella[m], E.V. Demidova[k], A. Denisiv[j], S. Dinter[m], A. Di Vacri[a], A. Domula[c], V. Egorov[d], F. Faulstich[m], A. Ferella[r], K. Freund[q], F. Froborg[r], N. Frodyma[b], A. Gangapshev[j], A. Garfagnini[n,o], S. Gazzana[f,a], R. Gonzalea de Orduna[e], P. Grabmayr[q], K.N. Gusev[l,d], V. Gutentsov[j], W. Hampel[f], M. Heisel[f], S. Hemmer[m], G. Heusser[f], W. Hofmann[f], M. Hult[e], L.V. Inzhechik[j], J. Janicsko[m], J. Jochum[q], M. Junker[a], S. Kionanovsky[j], I.V. Kirpichnikov[k], A. Klimenko[d,j], K-T. Knoepfle[f], O. Kochetov[d], V.N. Kornoukhov[k,j], V. Kusminov[j], M. Laubenstein[a], V.I. Lebedev[l], B. Lehnert[c], D. Lenz[m], S. Lindemann[f], M. Lindner[f], I. Lippi[o], X. Liu[p], A. Lubashevskiy[f], B. Lubsandorzhiev[j], B. Majorovits[m], G. Meierhofer[q], I. Nemchenok[d], C. O'Shaugnessy[m], L. Pandola[a], K. Pelczar[b], G. Pivato[o], F. Potenza[a], A. Pullia[i], S. Riboldi[i], F. Ritter[q], C. Rossi Alvarez[o], C. Sada[o], J. Schreiner[f], B. Schwingenheuer[f], S. Schönert[f], M. Shirchenko[l,d], H. Simgen[f], A. Smolnikov[d,j], L. Stanco[o], F. Stelzer[m], M. Tarka[r], A.V. Tikhomirov[l], C.A. Ur[o], A.A. Vasenko[k], A. Vauth[m], O. Volynets[m], M. Weber[f], M. Wojcik[b], E. Yanovich[j], P. Zavarise[a], S.V. Zhukov[l], D. Zinatulina[d], F. Zocca[i], K. Zuber[c], G. Zuzel[b],

[a]) INFN Laboratori Nazionali del Gran Sasso, LNGS, Assergi, Italy
[b]) Institute of Physics, Jagellonian University, Cracow, Poland
[c]) Institut für Kern- und Teilchenphysik, Technische Universität Dresden, Dresden, Germany
[d]) Joint Institute for Nuclear Research, Dubna, Russia
[e]) Institute for Reference Materials and Measurements, Geel, Belgium
[f]) Max Planck Institut für Kernphysik, Heidelberg, Germany
[g]) Dipartimento di Fisica, Università Milano Bicocca, Milano, Italy
[h]) INFN Milano Bicocca, Milano, Italy
[i]) Dipartimento di Fisica, Università degli Studi di Milano e INFN Milano, Milano, Italy
[j]) Institute for Nuclear Research of the Russian Academy of Sciences, Moscow, Russia
[k]) Institute for Theoretical and Experimental Physics, Moscow, Russia
[l]) Russian Research Center Kurchatov Institute, Moscow, Russia
[m]) Max-Planck-Institut für Physik, München, Germany
[n]) Dipartimento di Fisica dell'Università di Padova, Padova, Italy
[o]) INFN Padova, Padova, Italy
[p]) Shanghai Jiaotong University, Shanghai, China
[q]) Physikalisches Institut, Eberhard Karls Universit"at Tübingen, Tübingen, Germany
[r]) Physik Institut der Universität Zürich, Zürich, Switzerland

Spokesperson: S. Schönert
(*Stefan.Schoenert@mpi-hd.mpg.de*)
Deputy Spokesperson: C. Cattadori
(*Carla.Cattadori@lngs.infn.it*)
Technical Coordinator: K.T. Knoepfle
(*Karl-Tasso.Knoepfle@mpi-hd.mpg.de*)

URL: `http://www.mpi-hd.mpg.de/GERDA/`

Contents

1 Phase I detectors and R&D for liquid argon instrumentation

The activities of task group one (TG-01) focused during the last six months on *i)* the deployment and operations of the non-enriched germanium diodes in GERDA and the studies related to the ^{42}Ar/^{42}K signal, *ii)* the operation of a natural BEGe detector in the GERDA low-background test-stand LArGe in order to study the background reduction achievable with a liquid argon scintillation veto combined with pulse shape analysis, and *iii)* on the ^{42}Ar/^{42}K signal in LArGe. The details of the activities of *i* and *iii*, and the achieved results are reported in the internal GSTR note on the first data taking period with natural detectors, which is available to the LNGS SC. Here we briefly summarize the results obtained with the BEGe detector operated in LArGe.

1.1 Background suppression of a BEGe detector in LArGe

The 80 mm diameter BEGe (s/n: b 09001) with 878 g mass, previously operated in the GDL liquid argon test stand [1], has been deployed in the LArGe test stand. The energy resolution of the detector inside LArGe, coupled to a (non-low background) CC2 front-end board was 2.0 keV (FWHM) at 1.33 MeV and 1.6 keV (FWHM) with the pulser. The operational voltage was 4000 V and the leakage current stable at about 4 pA.
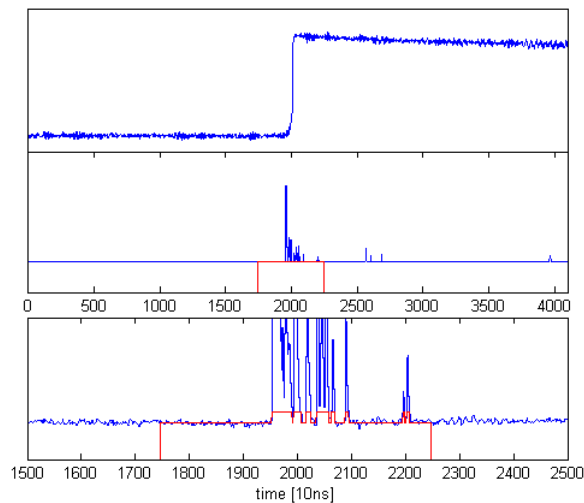
Figure 1: Coincident signals of the BEGe detector (top canvas) and the PMT liquid argon scintillation (middle, zoom in bottom canvas) in LArGe.

The purpose of this measurement campaign was to study the achievable background suppression combining the liquid argon scintillation veto and the pulse shape analysis employing the A/E method. For this purpose, a comprehensive series of measurements was performed employing ^{228}Th, ^{226}Ra,^{60}Co, ^{137}Cs gamma sources located both close to

the crystal inside the liquid argon and outside of the cryostat. The germanium and liquid argon scintillation data were recorded with a FADC system and stored for the off-line analysis. Fig. 1 displays the FADC traces of the BEGe and the PMT signal

Figure 2 displays the detector response of a ^{228}Th gamma source for two distances between source and detector. In the top figure, the source is external to the cryostat at 50 cm distance. In the bottom figure, the source is located inside the liquid argon, a few cm away from the crystal. The events with energies above 2.6 MeV in the lower figure are summation events. The line close to 3 MeV (top and bottom) is the pulser signal. The red histograms are achieved after applying the liquid argon scintillation veto cut. Given the characteristic de-excitation with multiple-gamma emission following the ^{208}Tl decay, the suppression factors depend on the source location. This can be used as a diagnostic tool to identify the location of background sources.
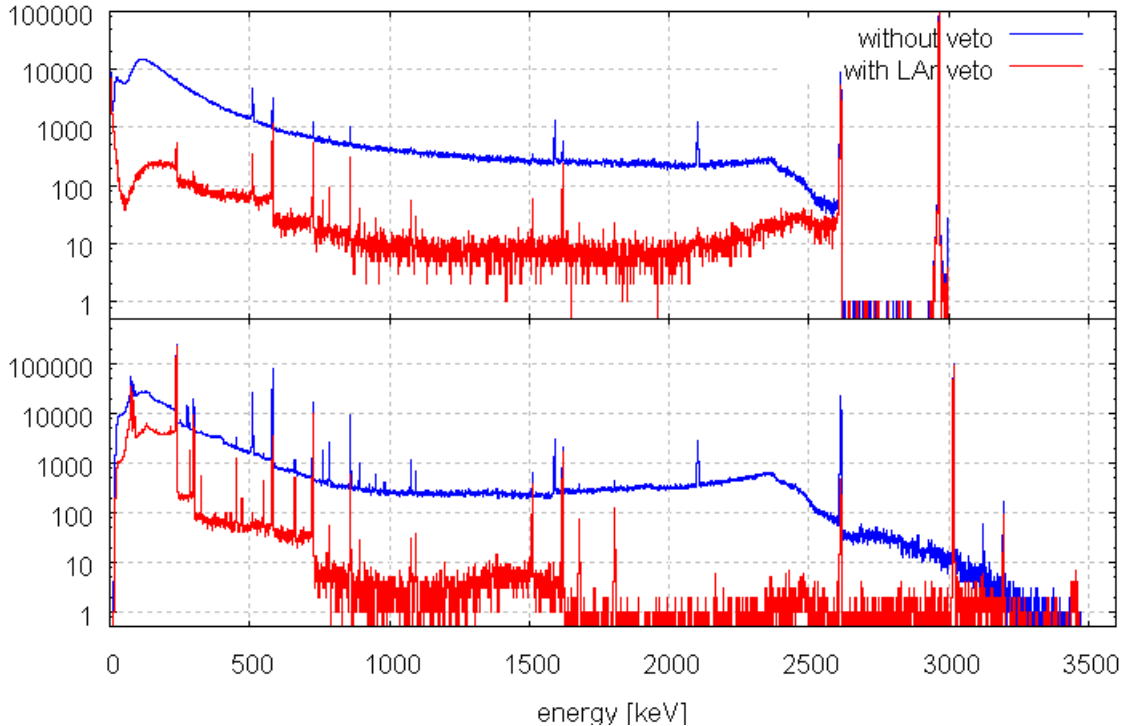
Figure 2: Response of a BEGe detector for a far (top) and near (bottom) ^{228}Th source. The blue histograms are prior and the red after applying the liquid argon veto cut. The peak around 3000 keV is the pulser signal.

While the liquid argon scintillation veto discriminates background events with energy deposition *external* to the germanium diode, pulse shape analysis of the germanium detector signal provides information whether the energy deposition was point-like or multi-site

5

internal to the germanium diode. We therefore performed a pulse shape analysis following our A/E method [2] of the BEGe detector signal. The resulting histograms are shown in Fig. 3.
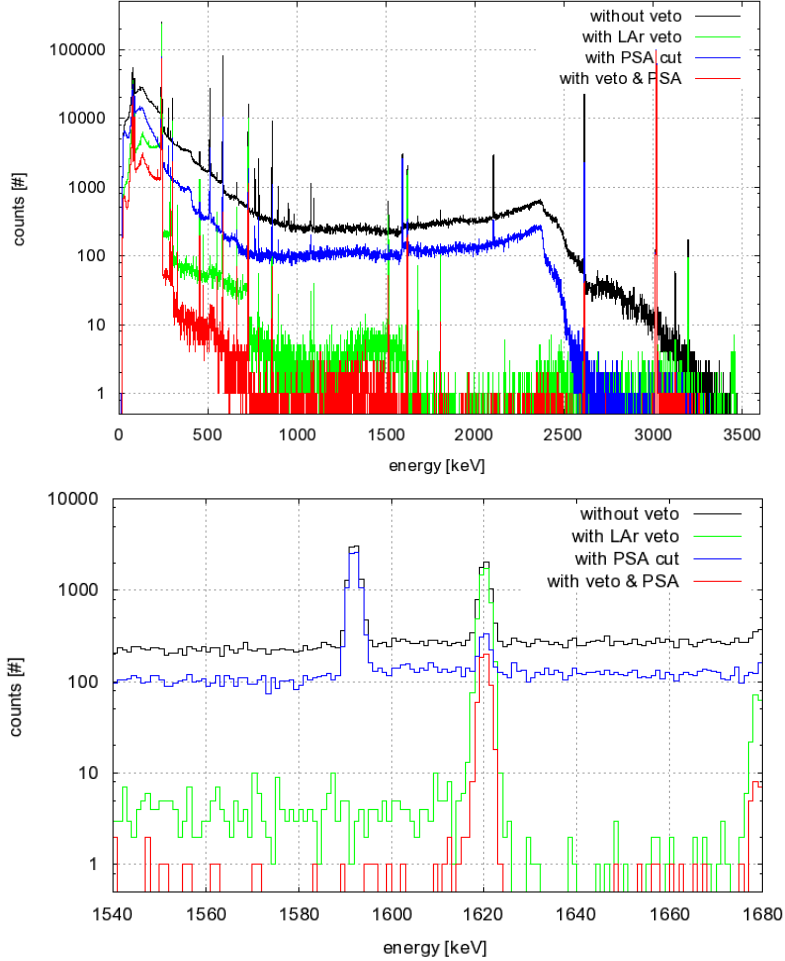
Figure 3: Response of a BEGe detector to a ^{228}Th source irradiation in LArGe. The spectrum prior analysis cut (black), with liquid argon veto (green), with A/E pulse shape analysis (blue), and with simultaneous application of liquid argon veto *and* A/E pulse shape analysis (red). The bottom figure is a zoom on the double escape peak (mainly single-site) of the 2614 keV line at 1592 keV and the 1620 keV full energy (mainly multi-site) line. The total suppression at $Q_{\beta\beta}$ is $(1.6 \pm 0.7) \times 10^{-4}$.

In these measurements, we achieved a background suppression factor of $(1.6\pm0.7)\times10^{-4}$ at $Q_{\beta\beta}$ for a near ^{228}Th source using simultaneously the liquid argon scintillation and the pulse shape information of the BEGe detector.

6

2 Phase II Detectors

Since the last scientific committee meeting, a milestone was reached and a very important decision was made:

- The collaboration has decided to pursue the BEGe detector technology for Phase II, and
- the purification of the ^{enr}Ge for Phase II was completed successfully with very high yield of 6N material.

We give more details on these items below, as well as give updates on the crystal pulling activities at IKZ, on procurement and test of BEGe prototypes and on R&D with segmented n-type detectors.

2.1 Phase II detector decision

As has been documented in previous reports, the BEGe detector production chain starting from GeO_2 from ECP, reduction and purification at PPM Pure Metals, GmbH, zone refining and crystal pulling at Canberra (Oak Ridge) and detector production at Canberra (Olen) was successfully tested. To date, five BEGe detectors have been produced from ^{dep}Ge ('waste' material resulting from the enrichment procedure at ECP). The performance of these detectors has been excellent both for energy resolution and background suppression via pulse shape analysis. The active background rejection achieved with these detectors is at least as good as that achieved with segmented detectors. The fewer electronics channels required compared to segmented detectors implies that the ambient background levels should be smaller, so that the overall performance is expected to meet our Phase II goals. The costs for these detectors is also estimated to be smaller than for the n-type segmented detectors. The collaboration has therefore decided to make the BEGe detectors the nominal choice for Phase II, and negotiations have begun with Canberra on a contract for production of ca. 20 kg of BEGe detectors. Our goal is to have the first batch of Phase II diodes available by the end of 2011.

We anticipate having of order 15 kg of ^{enr}Ge remaining after this production run. This material will need re-purification, and this is expected to take place at PPM. We will pursue our crystal pulling research activities at IKZ. If the required crystal quality is reached, producing a further batch of detectors from IKZ crystals would be our favored path for processing this remaining material. The detector technology for this production would be determined based on the performance of the BEGe detectors in GERDA.

2.2 Purification at PPM Pure Metals GmbH

The 53.3 kg enriched GeO_2 was stored in the SCK CEN Mol (Belgium) underground lab from April 2006 - March 2010. On the 8th of March 2010 it was transported to Goslar (Germany) for reduction and purification at PPM Pure Metals in Langelsheim

(near Goslar). For the time of the processing the material was stored underground in the Rammelsberg mining museum in Goslar.

The total amount of GeO_2 was reduced to Ge metal and purified with zone refinement. The yield of the chemical reduction was around 98%.

The first step was to reduce the GeO_2 to Ge metal. Once the reduction produced enough material the zone refinement could be done in parallel. To increase the yield of the purification the low resistivity ($< 50\,\Omega$cm) part of the refined ingot was cut off and was zone refined again. This procedure was repeated until the left over material was insufficient to fill a zone-refining boat. At the end of the zone refining process, only a half ingot, 1.16 kg, remained that did not qualify as 6N material. The reduction and zone-refinement of the enriched material was completed on April 29th, 2010.

The overall yield of germanium metal was 97 %. This is only slightly less than the 98% yield of the reduction. Losses occurred during chemical etching and cutting of the ingots. In total 36.6 kg Ge metal was produced out of which 35.4 kg is 6N material. The overall yield of 6N material was about 94 %.

To reduce the cosmogenic activation only the material that was actually being processed was above ground. The finished ingots were taken back in the mine within the same day. The total average exposure during the processing including transport from Geel was 125.97 h or 5.25 days.

At the end of the processing the material was packed in two aluminium boxes and left underground in the Rammelsberg mine to await crystal pulling and detector fabrication.

2.3 Update on crystal pulling at IKZ

The development of a reliable high quality crystal pulling setup at IKZ continued using depleted Ge from ECP, reduced and zone refined at PPM. To improve the quality of the input material for the crystal puller, we produced multiply zone refined ingots at PPM. This was done using the leftover of previous crystal pulling tests and 10 kg of depleted germanium was sent to PPM for reprocessing. In total 30 zone refinement passes were done on each ingot, about three times more than during the usual procedure. The purified material was delivered to IKZ in May.

In the crystals grown from the multiply zone refined material the dominant impurities are Al and P with a concentration of the order of $10^{11}/cm^3$. All crystals show predominantly p-type conductivity. The impurity level in the crystals from the multiply zone refined material is on average better, indicating that this approach holds promise for future improvements.

The dislocation density was measured on some crystals grown in the past. It was found that typically is between 10^4 and $10^5/cm^2$ about one or two orders of magnitude higher than what is needed to produce HPGe detectors. In the future the temperature and the growing speed will be adjusted to produce the right number of dislocations.

Future plans to improve the crystal purity include installing a quartz tube inside the puller to reduce the volume from where impurities can diffuse into the crystal. The first results with this method are expected in October.

2.4 Update on BEGe detector procurement and tests

Two more thick-window p-type BEGe detectors produced from depleted germanium have been produced and tested since the last LNGS SC meeting. In total, five diodes have been produced from the depleted germanium material so far. Four of them have been mounted into vacuum cryostats while one (from P81878AA) has been tested only for it's performance as a diode because of it's bevel shape. Table 1 summarizes the main characteristics of these detectors.

Table 1: Summary table of thick-window BEGe diodes produced from depleted germanium material. The diode made from the seed end (AA) of P81878 has a strong bevel shape and only its diode characteristics have been measured.

Crystal	Slice	Batch	s/n	Diam./Length (mm)	Mass (g)	FWHM (keV)
P81878	AA	1st	b 11008	66.0/28.0	400	N.A.
P81890	CC	1st	b 11009	74.5/33.0	760	1.61
P81890	DD	1st	b 11039	74.0/32.0	700	1.66
P81878	BB	2nd	b 11123	75.4/31.0	734	1.6
P81886	BB	2nd	b 11124	74.5/41.0	930	1.7

The selection of the crystal slices was based on the particular characteristics of the crystal. With the P81878AA slice we investigated whether diodes can be produced from the seed end of the crystal. Only after removal of additional material from the conical part, a diode could be produced successfully. The diodes made from P81890CC and from P81890DD were both from the 1st batch. They were produced according to the usual design criteria by the manufacturer though P81890DD is from the tail end and slightly bevel shaped. Such geometry is usually not used in the commercial BEGe detector production. The crystal slices P81878BB and P81886BB were dimensioned and cut in a non-standard way in order to optimize the overall detector mass yield. Less crystal skin was removed for P81878BB, while the length of P81886BB had been increased given the impurity levels of this crystal slice. All detectors show excellent energy resolution and pulse shape characteristics. The analysis characterization of the detectors of the 2nd batch is still ongoing.

2.5 Update on n-type segmented detector R&D

A production chain for producing polyethylene napthelate (PEN) cables is being investigated as a possible low-background readout for segmented n-type germanium detectors. The PEN film can be produced with low contamination levels; $^{238}U/^{226}Ra < 2$ mBq/kg, $^{232}Th < 1.4$ mBq/kg, and $^{40}K < 3.6$ mBq/kg have been measured using ultra low level gamma spectrometry. From this substrate a flexible printed circuit (FPC) has been produced for readout of the germanium detectors in a design layout that has been proven by

production on a polyimide Kapton substrate.

A PEN readout cable has been installed on one of the 18-fold segmented prototype detectors. The detector used has one segment that draws increased leakage current. Therefore the energy resolution of the corresponding segment and of the core were deteriorated. The detector has been operated in liquid nitrogen with the PEN readout cable. A picture is shown in Fig. 4a.) The spectrum recorded from a ^{60}Co source on one of the typical segment channels is shown in Fig. 4b.) With the exception of the core channel and channel 15, the broken segment that draws a high leakage current, the obtained energy resolutions at 1.3 MeV are with 3 keV to 5 keV commensurate with the resolutions recorded with the equivalent cable produced on a polyimide substrate as published earlier [3].
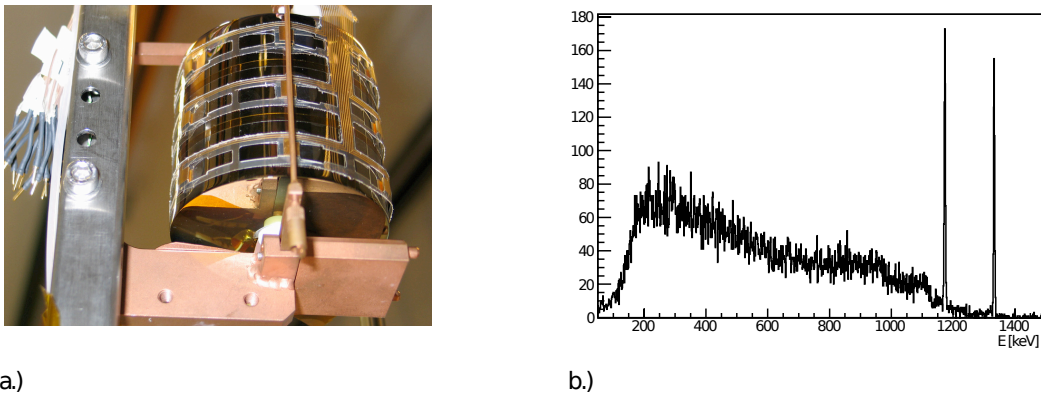

a.)   b.)

Figure 4: a.) Photograph of the 18-fold segmented n-type HPGe detector with PEN cable for signal transmission installed, and b.) the ^{60}Co spectrum as recorded from one of the segments of the detector.

3 Cryostat and infrastructure

The operation of the cryostat is very stable since it was filled in December 2009. The vacuum pressure is stable at 3×10^{-8} mbar, the active cooling with liquid nitrogen is working such that no argon was refilled since January 2010, the pressure regulation keeps the absolute pressure at 1.2 bar with a variation of less than 50 mbar and the monitoring and PLC control is running continuously.

During a refilling of the nitrogen storage tank, the operator let the tank pressure rise above 10 bar which triggered the safety valve on our transfer line and cause a spill of liquid nitrogen. This the only incident since the operation started.

The water drainage is controlled by the cryostat PLC. In a test performed in May we managed to empty the entire water tank in less than two hours while keeping the maximum flow rate below 70 l/sec. This is achieved by adjusting the opening angle of a butterfly valve which was added in the drainage pipe. The only hardware piece missing is a drainage pipe to the "GNO" pits to reduce the time for emptying further.

4 Detector loading infrastructure

4.1 Clean room on top of the tank

The clean room has started operation in 2009 and is running stably since. The main parameters defining its conditions are monitored online and can be viewed at `http://ge-gate.lngs.infn.it/`

A screenshot of the clean room online monitor is shown in Fig. 5. Thanks to the interface to the slow control, histories of all parameters can be displayed.
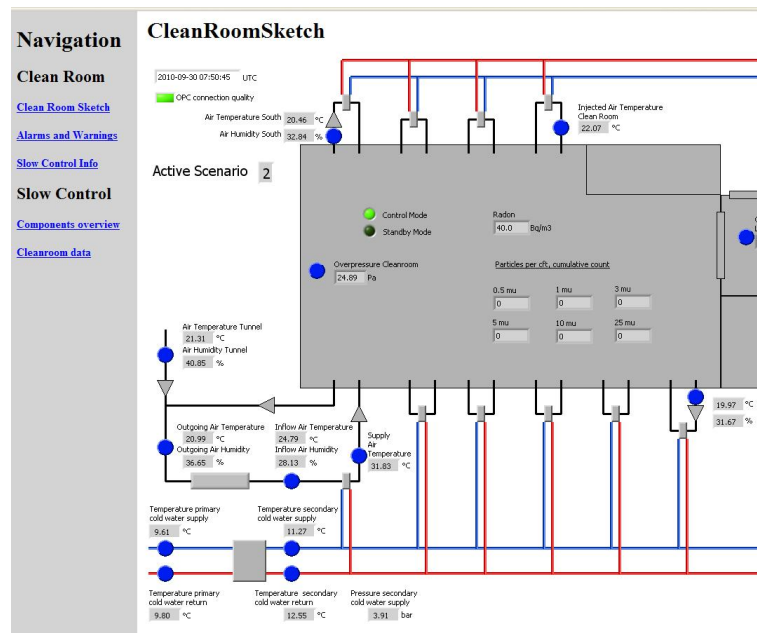

Figure 5: Screen shot of the clean room online monitor.

4.2 The commissioning lock system

The infrastructure to lower three detectors into the cryostat has been installed in hall A in March 2010. The associated PLC as well as gas- and vacuum system were installed in April and May 2010. To test the system a first detector dummy was released into the liquid Argon tank on 10th of May 2010. The cable arm with three HPGe detectors is used for the first background measurements since.

4.3 Second cable arm

A second cable arm is presently being prepared at MPI für Physik in Munich, Germany for installation in hall A. This cable arm will have enough space to install three strings of detectors.

The additional weight requirements due to the increase from one to three strings and the increased number of signal transmission and HV lines made a modification of some components of the linear pulley system necessary. Instead of the steel wire holding the movable deflection pulley a steel band on a modified drum was designed, tested and implemented. Stress tests revealed that even a damaged steel rope does not break at a weight of 200 kg, which is roughly a factor of five safety margin.

Signal transmission lines and HV cables have been interwoven with PTFE thread into flat band cables. A flat steel band was included inside the cable chain as a gliding surface for the cable bundles. With this solution, the required number of cables can be implemented into the cable chain.

Extensive tests were performed at the MPIP to guarantee reliability of the system. A cable chain with all cables installed was mounted on a mock-up system and lowered sixty times. The flat band cables as installed into the cable chain are shown in Fig. 6. No indication of deterioration of performance could be seen. One of the flat band cables with 5 HV lines used in the stress test has been submerged into liquid nitrogen and warmed up for 30 cycles. Subsequently it was put under HV and leakage current was measured. No sign of performance deterioration was seen.

The screening measurements of the cables and the interwoven PTFE revealed that the material is suitable for usage in phase I.

Final installation and test of the three string cable arm at Max-Planck-Institut für Physik in Munich will be finished by November 2010. Installation on the GERDA cryostat will begin by the end of the year 2010.

4.4 Final lock system

After completion of measurements with the existing HPGe diodes up to 30 BEGe detectors with a mass of roughly 0.7 kg each made from the ^{enr}Ge material need to be installed into the GERDA tank. Provided the yield in detector production is high and/or additional enriched/depleted material might be available the number of detectors might increase to up to 50 or more detectors. The final lock system is designed for installation of up to 16
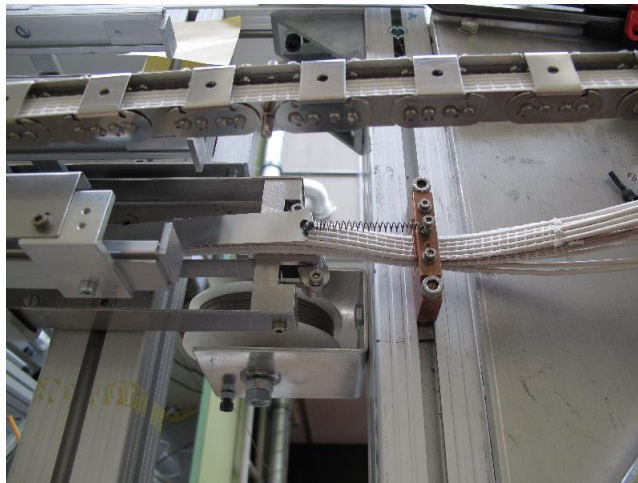
Figure 6: Full set of cables for three string lock in cable chain on mockup. Two HV flat cables with 5 HV lines, three signal flat cables and a steel band are installed into the cable chain. The flat cables are strain relieved onto the top of the cable chain. The steel band protects the flat cables from being scratched by the cable chain segments.

strings housing in total up to 80 detectors with dimensions according to 18-fold segmented prototype detector design.

As the baseline design has been changed from segmented to BEGe-type it is presently being investigated what design changes need to be done. Changes to simplify handling of the detectors inside the lock are being considered:

- reduction of string positions to the necessary minimum,
- possibility of reaching inside the lock system during installation,
- implementation of system for measurement of real string position.

Table 2: Report of the γ-ray screening of the CC2 circuit with minimal number of components (no pins, no NP0 capacitors). Upper limits are given at 90 % CL.

isotope	activity
^{232}Th chain	
^{228}Ra	(0.20 ± 0.11) mBq/CC2
^{228}Th	(0.14 ± 0.06) mBq/CC2
^{238}U chain	
^{226}Ra	(0.29 ± 0.10) mBq/CC2
^{234m}Pa	< 1.3 mBq/CC2
^{235}U	< 0.13 mBq/CC2
^{40}K	(1.9 ± 0.7) mBq/CC2
^{137}Cs	< 42 μBq/CC2
^{60}Co	< 56 μBq/CC2

5 Status of Front End Electronics

We focused on the minimization of the radioactivity of the 3-ch circuit whose previous realization was not completely satisfactory (350 μBq of ^{232}Th); the PCBs were produced once more reducing further the PCB dimensions and optimizing the geometrical dimensions of the Cu trace capacitors. Two Cu trace capacitors can be put in parallel, in order to match a couple of relevant dynamic range while avoiding the use of SMD ceramic capacitors. All the SMD components were remeasured. The final results are within the expectation. Figure 7 shows the circuit fully populated, while Table 2 reports the results on the radioactivity in terms of ^{238}U, ^{232}Th, ^{40}K etc. measured by γ-ray spectrometry.
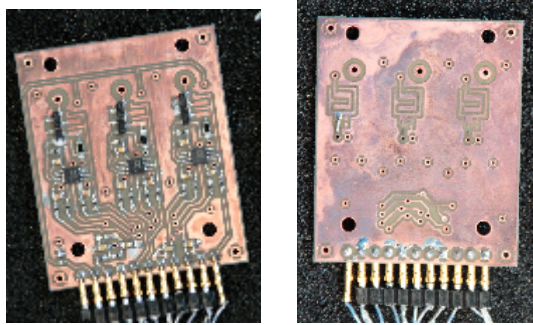

Figure 7: The CC2 circuit (front and back) in its definitive form: in the back view the trace capacitors are visible

The ^{232}Th and ^{238}U contents are ~ 170 μBq and ~ 290 μBq respectively for a 3-ch PCB, to be compared with the reference values from simulations of 500 μBq and 2.5 mBq, respectively, leading to a background contribution of few 10^{-3} cts/(keV·kg·y) for a PCB

placed at 30 cm from the top detector (3 string simulated). We believe that this is the minimal value obtainable with the present architecture. As soon as the measurements from a new batch of soldering wire will be available, we will mount 8 PCBs with the available screened components.

One of the new low activity PCBs has been installed on 14th August in LArGe to read out the GTF detector, and it allowed the reduction of the background of a significant factor.

6   DAQ electronics and online software

6.1   DAQ systems

Since June, the first detector string is operating in GERDA. While the first data taking was done with a multi channel analyzer (MCA), we are now taking data with a FADC system. We have tested both systems: the one using the commercial SIS3301 VME modules and the custom-built system. The resolution achieved with these systems are similar now (typically between 4.5 and 6 keV FWHM for the 2.6 MeV ^{208}Tl line) but somewhat worse than the one measured with the MCA (3.8-4.5 keV). The most likely reason is the low gain of the preamplifier of 0.55 mV per MeV energy deposition. This will be improved soon. For the understanding of the background these performance numbers are acceptable.

For the custom-built system, the graphical user interface was improved. The setting of trigger thresholds and monitoring of baselines to measure detector leakage currents was finalized.

The muon DAQ is running as well and providing a veto signal which is included in the diode readout stream. The final integration between the muon and germanium readout will take place when the background data taking is finished.

Still to be done is the storage of run based information like trigger settings and rates in the slow control database.

6.2   Slow Control and Network infrastructure

The underground GERDA network infrastructure has been enriched with a new server (GERDAServer tier0) with the following characteristics:

- dual Xenon 5520 CPU (1.86 GHz);
- 12 GBytes RAM (6 × 2 GBytes);
- RAID Adaptec 5805 controller;
- 8 SATA II disks, 2 TBytes each, 7200 RPM (server edition).

The disk space has been configured in RAID 5 with two partitions:

- 100 Gbytes for the OS (Debian Etch);
- 14 TBytes for data (xfs file system).

The data partition is exported via NFS and used to store Ge DAQ data and Veto DAQ data files. Batch scripts were started to copy files to the LNGS computing center.

The integration of the various sub-components has carried on. With respect to the last report (April 2010) the following components were integrated: water loop, temperature sensors of the room containing the Ge electronics and DAQ, VME and NIM crates. For example, Fig. 8 exhibits the values of temperatures registered in the rack hosting the Ge DAQ.
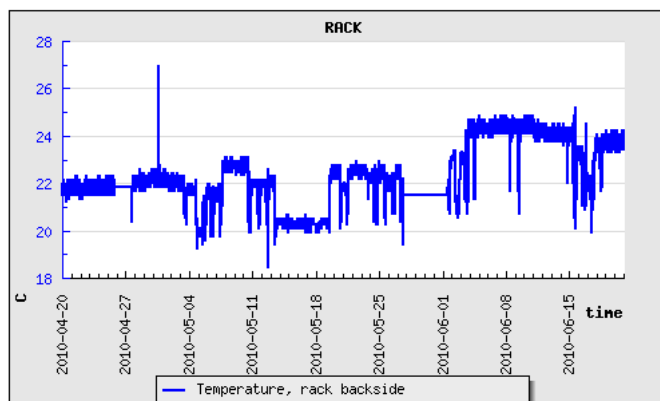

Figure 8: Ge DAQ rack temperature versus time.

At the present time, integration is in progress for the Low Voltage (LV) modules of the FE electronics and the HV of the Ge diodes. Fig. 9 shows a snapshot of the dedicated GUI for the remote control of the LV power supplies of the FE electronics.

Germanium detector High Voltage control and monitoring software has been designed and is currently under testing in the GERDA underground experiment. The left part of Fig. 10 shows a picture of the HV control board, hosted in a NIM module, which is a custom design based on an embedded Linux board with ARM CPU. The board, running a LINUX operating system, has an autonomous power line completely decoupled from the NIM crate power supply, is directly connected to the Ethernet and reads the CAEN N1471 HV power supplies (Fig. 10, right part) through a dedicated USB connection. Integration in the GERDA slow control environment (with alla data stored in the central database) is ongoing and a custom WEB interface is being developed for the GERDA experts to read and modify the Germanium detectors High Voltage parameters during data taking.
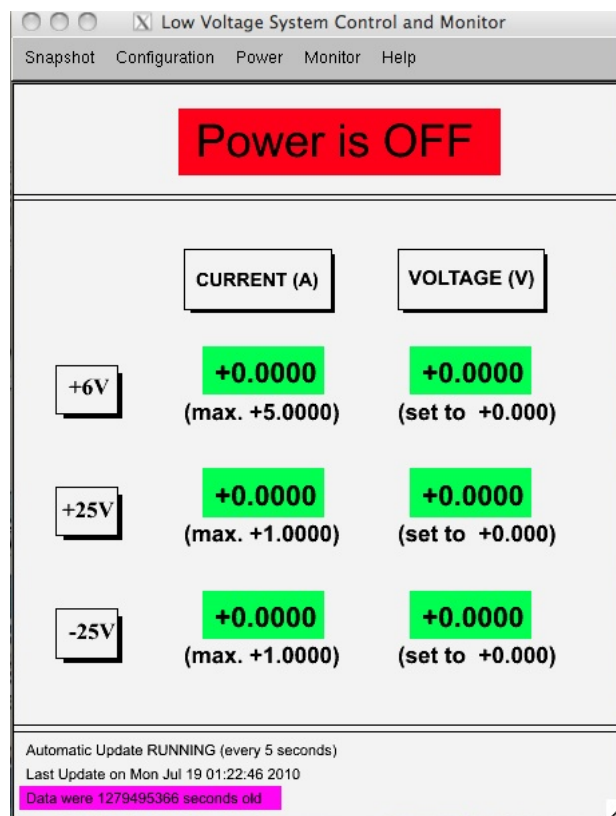
Figure 9: Graphics interface for the remote control of the LV power supply of the Ge FE cards.

Figure 10: The NIM module containing a small board (left side) controlling the HV CAEN N1471 modules (right side) via USB/serial interface.

7 The Muon Veto

7.1 Repair and calibration

Due to the water drainage for a safety test the photomultipliers of the Cerenkov muon veto [4] could not be tested when submerged immediately after the installation in 2009. Only in early summer 2010 the water level could be raised above 6 m to submerge all PMTs. As it turned out, one of the cables was damaged during installation, one PMT was not working. The latter could be replaced by cutting the cable and substituting a spare PMT with the equivalent length of cable. The damaged cable could not be replaced due to problems of access and this PMT remains out of order until repair during a longer shut down period. The Monte Carlo simulation indicate that the loss of this PMT on the bottom of the water tank does not reduce the efficiency of the muon veto significantly. Even if a second PMT would be lost, the efficiency remains at a level of ∼99,4 %.

By use of the diffuser balls a calibration of the response of the PMTs was achieved. A low intensity was chosen to find the one-photon response and adjust the HV such that this intensity falls into channel 80 (-80 resp.) of the FADC for all PMTs. The good reflectivity of the VM2000 foils allowed to fire all PMTs in a single measurement with all five diffuser balls shining simultaneously. We are checking if more complicated procedures will be needed for refined tuning.

This adjustment was also part of the setup of the FADC and DAQ system provided originally by the MPI in Heidelberg. A quick commissioning of the DAQ was sufficient to establish the main features of the muon veto and to permit a first rough veto signal to augment the tests of the Ge-array. Presently, a low level trigger signal from the muon veto is fed into the DAQ of the Ge-detectors. No pulse heights are recorded, only the time correlation between the muon and the Ge-diode signals. Evaluating the coincidence gives an upper limit of the muon induced background events.

7.2 Test of trigger conditions

Several trigger levels have been tested during July and August [5]. We want to run with a low discriminator level, definitively below 1 photo electron. In order to avoid random coincidences due to noise we request a number of FADC to fire within a certain time. In Fig. 11 spectra from four conditions are displayed, every panel has two histograms, the multiplicity and a 2D plot showing the integral light deposited versus multiplicity. The left top panel shows the results for the lowest threshold (-10) and lowest multiplicity of 3 to take place in a time slot of 5 clock ticks (50 ns). On the left bottom panel the threshold is increased to -50 which amounts to about 60 % of the one-photoelectron intensity (-50/3/50) while for the right hand side also the multiplicity and the time windows have been increased; right top: (-10/6/60) and right bottom: (-50/5/60). The green histogram display all hits, while the red ones show the subset of data where at least one PMT of the pillbox was involved. The spectra are not normalized, however the time of measurement is indicated.

In all conditions one observes a clustering of multiplicities around low (<20) and high

values above 60. The integral intensities indicate that the former might come from natural or induced radioactivity with some undetermined contributions from noise, while the high multiplicities clearly show the light from the electro-magnetic shower due to the passage of the muon. A typical high multiplicity event is shown in Fig. 12, where the light intensity and arrival time are indicated via the color code and size. The left panel shows an event where the PMT fired in the pillbox only, the volume below the cryostat; the right one shows a high multiplicity event, which is attributed to a direct muon hit in the water.

The randomness of the low multiplicity contributions, or at least part of it is demonstrated in Fig. 13. The trigger time window is set around 1500 ns of the "HitTime". High multiplicity events are not found at earlier times in contrast to the lower ones, which are spread over the full range. Present investigations aim at the understanding of different possible contributions to this part. The rate of high multiplicity events is within a factor 2 of the expected muon rate.

The present veto trigger fed into the DAQ of the Germanium test array is set to a level of -10 and a multiplicity of 4 within a time window of 50 ns. The above considerations tell us that this rate of veto signals is too high compared to reality. Thus, this rate is a very high 'upper limit'. In case of few coincidences between the Ge and the muon signals, one reaches the conclusions that the background seen currently in GERDA can not be induced by cosmic muons.

The high multiplicity for events from muons is demonstrated by the Monte Carlo simulation. In Fig. 14 the PMTs are numbered from top to the pillbox with the latter having numbers 61 to 66. There are clear indications that a muon in the pillbox fires all 6 PMTs. The ridge at multiplicity 60 (and events below) indicates that some showers are seen only in the outside part of the water tank. Note, that the configuration of the PMTs in rings is resembled by the increased intensity observed as a grid in Fig. 14.

7.3   The Plastic Muon Veto

The plastic panels for the muon veto to be installed on top of the clean room are assembled in Dubna and are being prepared for shipment to LNGS via Tübingen for customs reasons.

In parallel we are going to perform in November a test with 7 panels on top of the clean room to explore the mechanical construction and check the slow control as well as the DAQ in connection with Ge data.
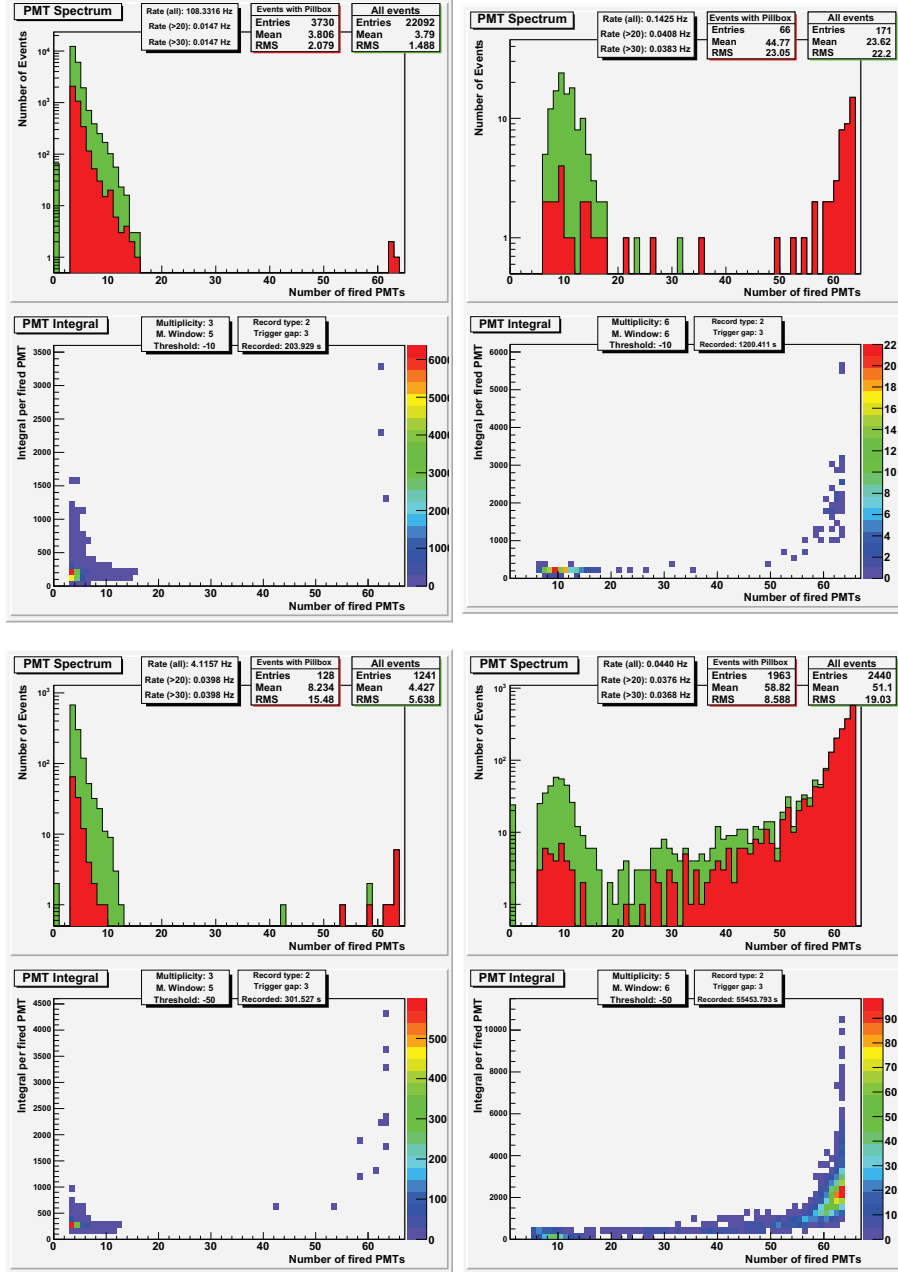
Figure 11: Multiplicity and integral light response for the Cerenkov Muon Veto for four trigger conditions. (see text)
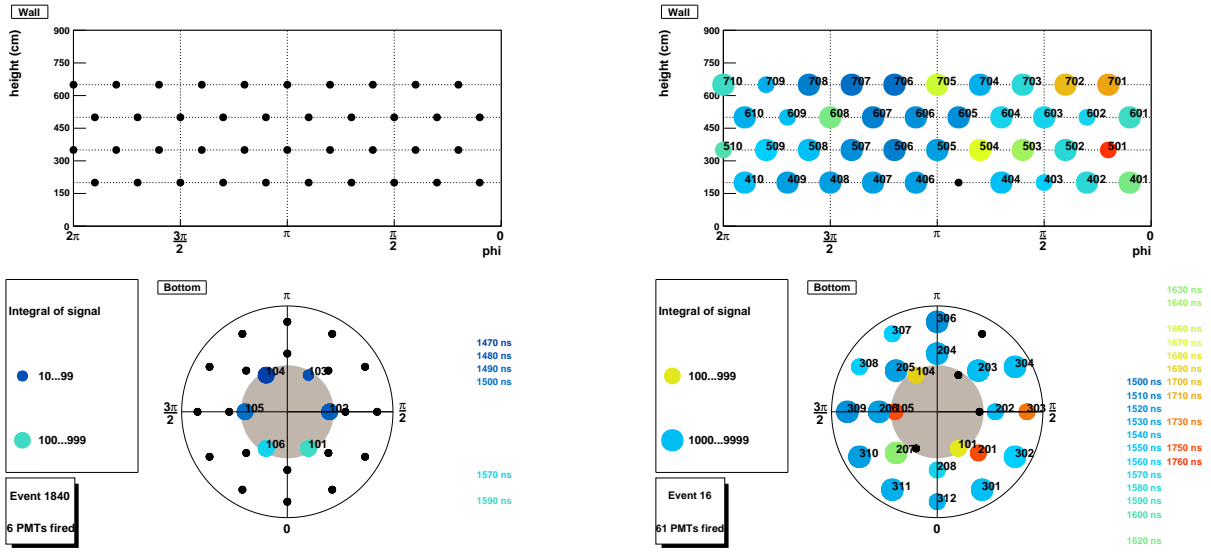
Figure 12: Two typical hit pattern of registered muons Left: signal in pillbox; Right: muon seen by almost all PMTs.
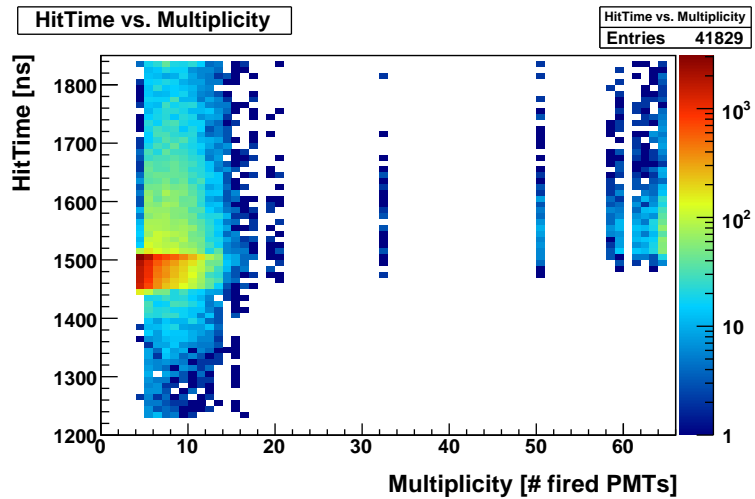

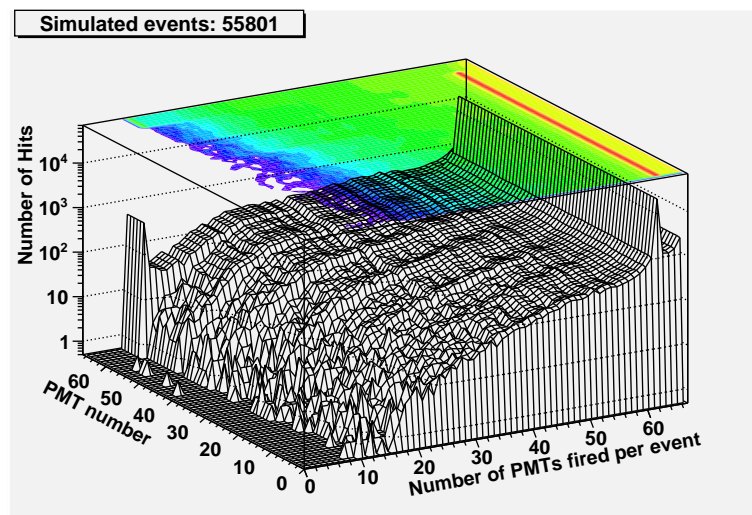Figure 13: Time versus multiplicity. (see text)

Figure 14: The result of the Monte Carlo Simulations for muons shows the multiplicity versus PMT involved. The PMTs of the pillbox are number 61 to 66.

8 Simulations and background studies

The main activity within the Task Group was the design, implementation and test of new software tools for data handling and analysis. A significant effort has also been placed in detailed Monte Carlo simulations to interpret the recent measurements with the 3-detector pilot string, and specifically the ^{42}K signal.

8.1 Data analysis algorithms and infrastructures

MGDO

As described in the previous report to the Committee, a major activity within the Task Group had been the development, test and upgrade of the MGDO (Majorana-GERDA Data Object) software library, which is maintained jointly with the MAJORANA Monte Carlo group.

The format defined in MGDO is meant to be used as a standardized format ("tier1") for easy sharing and readability of data files. All raw data collected within the GERDA activities (main GERDA setup, LARGE, characterization of BEGE detectors, etc.) are converted in an MGDO-based format, so they can be read and analyzed with the same codes, irrespectively of the original format.

In the last six months, a substantial effort in the MGDO development has been dedicated to the extension and improvement of general-purpose basic algorithms ("Transforms") for data analysis. Newly implemented algorithms include pulse fitting, baseline restoration, calculation of rise time, smoothing and deconvolution. Individual algorithms are intended to be used sequentially in a chain for complex data analysis (e.g. energy reconstruction), as discussed below.

GELATIO

A new dedicated C++ software package called GELATIO (GErda LAyouT for Input/Output) has been initiated and intensively developed in the past months. The main aim of GELATIO is to provide general and flexible GERDA-dedicated tools for the handling and analysis of data, starting from data files in MGDO format. While MGDO is uniquely a library, GELATIO contains executables that users can actually run and includes the information to decode all the raw data formats currently used in GERDA. GELATIO is an original development of the GERDA TG10 group.

GELATIO uses the approach of the ROOT-based TAM library [6] to achieve a completely modular analysis. The software contains several independent analysis modules, each one performing a well-determined and self-consistent task of the digital data analysis. This encompasses - e.g. - determination of the onset, reconstruction of energy (possibly according to different algorithms), calculation of the A/E ratio, calculation of rise time. Each module implements a chain of basic MGDO Transforms. Users can freely customize the number/type of active modules (as well as their internal parameters) for the analysis of a given data file. The choice of modules to be activated and of their parameters does
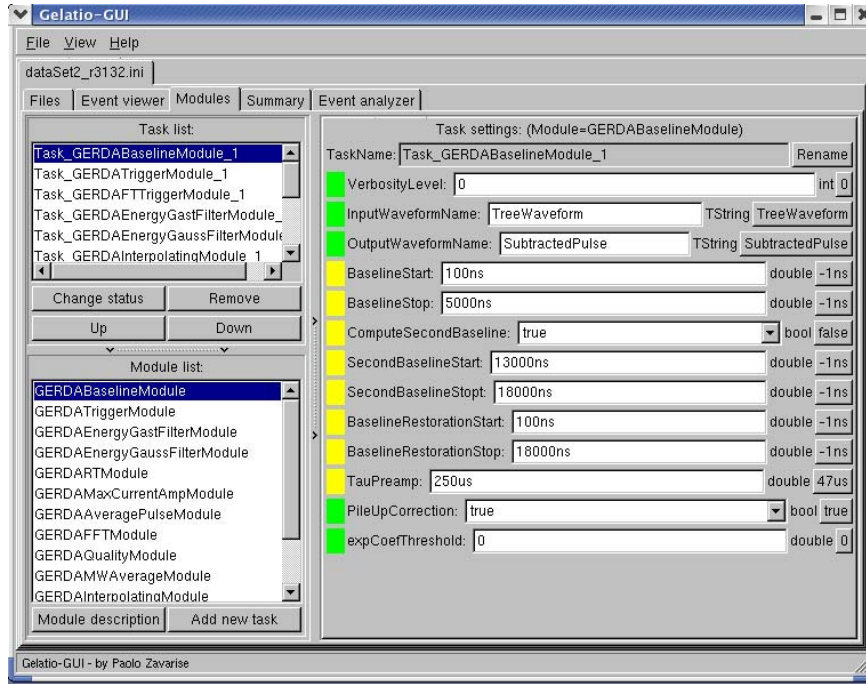
Figure 15: Screen-shot of the GELATIO graphical user interface. The interface allows to customize interactively each analysis run, by choosing: (1) the files to be processed (not visible in this screen-shot); (2) the analysis modules to be activated among the available ones (left panel); (3) the internal parameters of each active module (right panel).

not need any C++ coding, but can be done either in a human-readable ASCII file or via a ROOT-based graphical user interface (see screen-shot in Fig. 15). The general interfaces available in GELATIO allow users to code their own alternative modules (e.g. a different algorithm for energy reconstruction) and to plug them easily into the main analysis program.

Additional programs available in GELATIO include an interactive event displayer (see screen-shot in Fig. 16) and a converter of GERDA raw data (taken in any of the recognized binary formats in use within GERDA) in the general MGDO format ("tier0 to tier1 conversion"). The graphical user interface of the event displayer allows to show interactively the digitized traces of each event in a MGDO data file as well as temporary pulses produced in each intermediate step of the analysis (e.g. the trapezoid pulse, the baseline-subtracted trace, etc.). The event displayer is used for quality control of the DAQ and debugging of the analysis code.

During the last six months, the full analysis stream foreseen for the GERDA data (namely, acquisition → conversion in MGDO → analysis within GELATIO modules) has been tested and benchmarked with real data, collected with different DAQ systems (characterization of prototype BEGe detectors, GERDA pilot string data, LArGe data, etc.). While the software infrastructure is still in a phase of intense development, results obtained are satisfactory in terms of flexibility and user-friendliness.
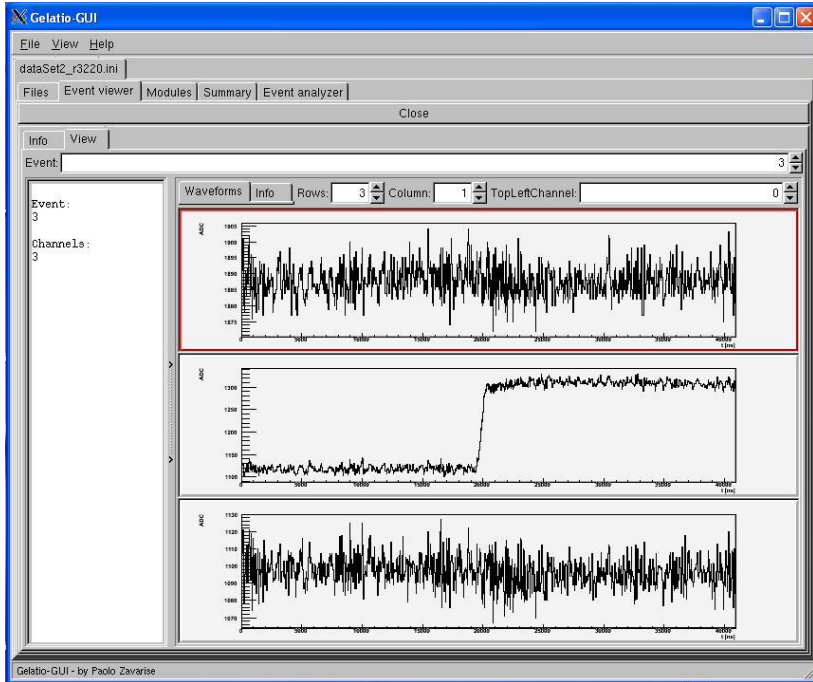
Figure 16: Screen-shot of the GELATIO interactive event displayer. The traces of all three channels are shown for the selected event.

8.2 Background studies from radioactive sources

^{42}K decay in liquid argon

The expected signal in the 3-detector GERDA pilot string due to the ^{42}K decay in LAr has been extensively simulated using the MaGe framework. The simulated geometry includes a realistic description of detectors, holders and supporting structures. The thickness of the dead layer has been assumed to be - for all detectors - 0.8 mm on the Li-drifted surfaces (n^+ contact) and 1 μm on the p^+ contact. It is assumed that ^{42}K are uniformly distributed in the LAr volume and that the ^{42}Ar-^{42}K rate is equal to the 90% upper limit found in the literature, namely $4.3 \cdot 10^{-21}$ g/g [7]. This corresponds to about 0.043 Bq per ton of LAr.

The simulated sum spectrum in the pilot string is displayed in Fig. 17; the spectrum extends up to the Q_β-value of the ^{42}K decay, 3.5 MeV. Given the assumptions above, the 90% upper limit for the total counting rate at the 1525 keV γ peak is

$$C_{1525} < 0.094 \quad \text{cts/(kg·d) at 90\% CL,} \tag{1}$$

which is clearly not consistent with what is observed in the real measurement. The large discrepancy between the measured and the expected rate indicates that at least one of the basic assumptions of the Monte Carlo simulation is not valid, namely either the limit of Ref. [7] is wrong (by at least a factor of four), or the ^{42}K decays are not uniformly distributed in LAr. Notice that the expected C_{1525} rate is only weakly sensitive to details of the geometry (e.g. the thickness of the dead layers).
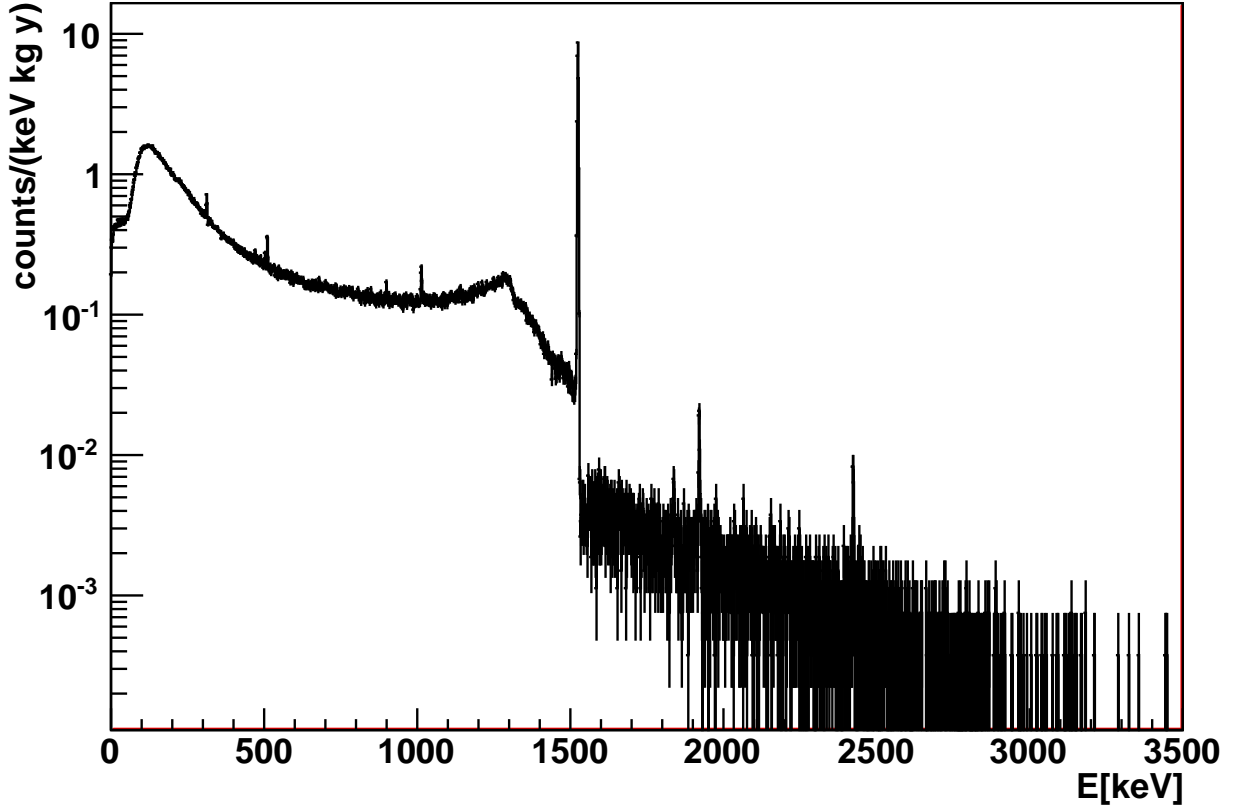
Figure 17: Simulated sum spectrum from ^{42}K in the pilot detector string in the assumption of uniform distribution with specific rate 0.043 Bq per ton of Ar (90% CL upper limit on ^{42}Ar contamination in liquid argon). No anti-coincidence cut has been applied.

The expected background index at $Q_{\beta\beta}$ for the pilot string is

$$B_{Q_{\beta\beta}} < 1.6 \cdot 10^{-3} \quad \text{cts/(keV·kg·y) at 90\% CL.} \tag{2}$$

Simulations show that the signal at $Q_{\beta\beta}$ is largely due to electrons penetrating in the crystals (about 93%); the remaining part is the Compton continuum from the rare ^{42}K γ-ray at 2424 keV ($I_\gamma = 0.02\%$). Indeed, electrons can penetrate in the detector only if they start from a very small region in the surrounding of the detector themselves, especially close to the p^+ surfaces, where the dead layer is extremely thin. The simulation results at $Q_{\beta\beta}$ are very sensitive to small details of the geometry, and specifically the thickness and extension of the dead layer. The predicted $B_{Q_{\beta\beta}}$ should be hence regarded as *qualitative* only, due to the large systematic uncertainty on the contribution from β electrons (which is dominant).

The extrapolation to the nominal Phase I array - with the assumptions described above

- gives a background index of

$$B_{Q_{\beta\beta}} < 1.7 \cdot 10^{-3} \quad \text{cts/(keV·kg·y) at 90\% CL,} \tag{3}$$

(with anti-coincidence cuts), which is well below the target background.

Notice that in Phase II the expected contribution of ^{42}K to the total background is substantially smaller, because different detectors will be used. In particular, BEGe detectors have a much smaller p^+ contact, so the signal at $Q_{\beta\beta}$ due to β electrons penetrating in the crystal will be strongly reduced with respect to Phase I.

At the moment, auxiliary Monte Carlo simulations are being run with different assumptions concerning the thickness of the dead layers and the localization of ^{42}K decays (e.g. concentration effects in the detector area, surface contamination, etc.). The main purposes is to help with the interpretation of the pilot string data.

Other isotopes

Other isotopes have been re-considered as possible background sources in GERDA Phase II, namely ^{22}Na ($Q_{\beta+} = 2.84$ MeV), ^{26}Al($Q_{\beta+} = 4$ MeV) inside the contacts and ^{110m}Ag ($Q_{\beta-} = 2.9$ MeV) in the electronic cables. It is found that the background index for all of them is below the required maximal value for the Phase II, given the measured or estimated activities.

9 Material screening

In the last few months the selection of radio-pure materials for front-end electronics was continued. New batches of previously selected low background components were purchased and measured. The results were in agreement with earlier measurements. Consequently, we have now the material in hand to mount all PCBs for the first phase of GERDA (see section 5).

Most of the other activities concerned radon measurements. The electrostatic radon monitor is working since September 2009 at LNGS below the GERDA tank without problems. The radon monitor is now connected to the exhaust line of the GERDA cryogenic tank via a mass flow controller and measures the radon content of the gaseous Ar. The flow is at the moment too low (0.3 l/min) to obtain meaningful results. A change of the connections will hopefully increase the flow through the monitor to 6 liters per minute. The Labview software which calculates the radon concentration based on the ^{214}Po and ^{218}Po peak intensity was updated and produces now a website displaying the radon concentration.

We have also investigated the dependency of the ^{222}Rn emanation rate on the temperature and on the environment by measuring the ^{222}Rn which is emanated from 4 % thorated thungsten welding rods. Due to traces of uranium in the thorium 100 welding rods yield a sufficiently high ^{222}Rn emanation rate into gaseous helium at room temperature (1.8 ± 0.1) mBq. When changing the temperature to -186 °C and still using gaseous helium as a carrier gas we could not measure any signal $(< 0.04$ mBq). In this case the ^{222}Rn is still emanated, but it sticks to the cold surfaces as could be demonstrated by a quick warm-up test after the measurement in which we found back almost all the ^{222}Rn. In a final series of tests we replaced the gaseous helium by liquid argon. The temperature remained unchanged (-186 °C), but now the environment is a cryogenic liquid instead of a cold gas. In this setup we found a ^{222}Rn emanation rate of (2.5 ± 0.1) mBq which is even higher than the room temperature result. A possible explanation is the larger stopping power of the liquid argon compared to the gaseous helium. ^{222}Rn which is recoiled during the ^{226}Ra-decay may be implanted to an opposite surface, if it only crosses gaseous helium. However, if it crosses liquid argon instead, it may be stopped and thus remains in the mobile phase.

10 Calibration

10.1 New sources, γ- and n-flux measurements

The first custom made ^{228}Th source has been calibrated at IRMM in Geel in May 2010, yielding an activity of (17.7 ± 0.5) kBq (the reference date being 1.04.2009, which is directly after the source preparation at PSI). The calibration procedure has been cross checked with a reference source from Eckert&Ziegler with a nominal activity of (25.5 ± 1.5) kBq (with 1.02.2010 as the reference date). For the commercial source, the activity measurement performed at IRMM is consistent with the value given by Eckert&Ziegler, with a relative

uncertainty that decreased to 3.1% with respect to the 5% value quoted by the company. Table 3 shows a summary of these results. Two additional custom sources were shipped to IRMM for calibration, before they were brought to LNGS for neutron flux measurements. The final calibration results for these two newest ^{228}Th sources are in preparation.

Table 3: Results of the ^{228}Th calibrations at IRMM

Source	Activity [kBq]	reference date
^{228}Th custom	17.7 ± 0.5	IRMM, 01.04.2009
^{228}Th commercial	26.5 ± 0.8	IRMM, 01.02.2010
^{228}Th commercial	25.5 ± 1.3	E&Z, 01.02.2010

In order to determine the neutron flux from all the sources and to cross check the neutron rates obtained with a ^{3}He detector (as reported in April 2010), a new LiI(Eu) detector has been tested in Zurich and brought to LNGS in August 2010. The neutron detection takes place via a prompt nuclear reaction in ^{6}Li with a Q-value of 4.78 MeV. The high Q-value results in an excellent γ-rejection performance. The detection efficiency of the LiI(Eu) detector reaches ∼100% for thermal neutrons. The thermalization of the neutrons takes place in a 5 cm thick polyethylene moderator in front of the detector, the optimal moderator thickness having been determined by measurements and Monte Carlo simulations. Fig. 18 shows the detector at LNGS, along with the inner and part of the outer polyethylene moderator (left) and calibration spectra taken with a gamma (^{137}Cs) and a neutron (AmBe) source above ground (right). The neutron capture peak on ^{6}Li is clearly visible.
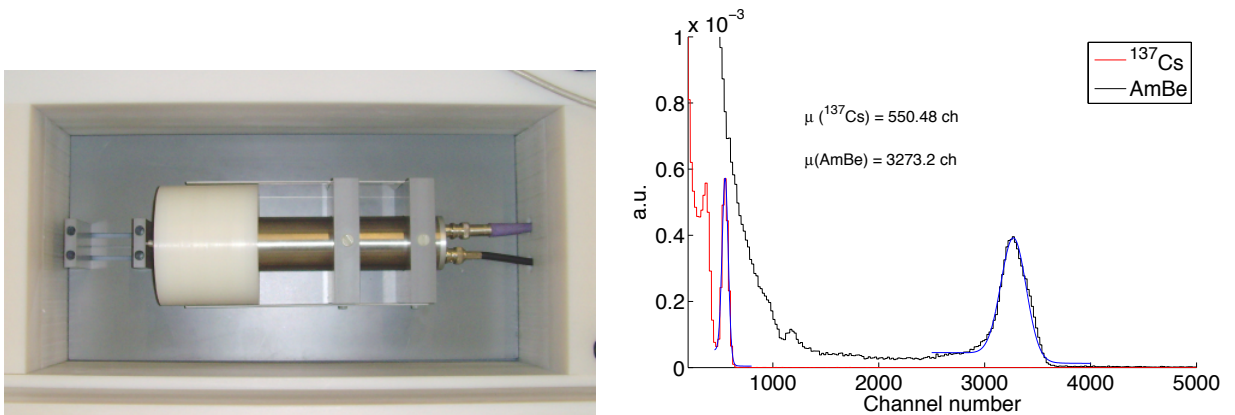

Figure 18:   (Left) LiI(Eu) setup at LNGS. The inner polyethylene will moderate the neutrons coming from the calibration source. The outer, borated polyethylene, provides a shield against the ambient neutron background; (Right) AmBe and ^{137}Cs calibration spectra taken above ground.

10.2 Calibration Source Lowering System

After the first on-site tests of the calibration source lowering system, the initial metal band that holds the Ta-absorber and the ^{228}Th source was cleaned. The cleaning revealed a very poor quality of the metal even after electropolishing, making it not usable for the experiment. It was replaced by the stainless steel band of the Meterdrive position measuring system, which is also used to control the detector position. The band has a length of 7 m and a thickness of only 0.1 mm to ensure that it fits into the pipe of the lowering system. The reading head necessary for the position determination is however too large for these pipes, hence four small metal pieces were installed at the nonius together with a hall sensor to count the number of turns when moving the source. A second load test was performed after these modifications.

The entire system was leak-tested in June 2010. At the first test the leak rate of $> 1 \times 10^{-5}$ mbar l/s was not satisfactory. Problems were found at the welding seams and the identified leaks closed provisorily using a two-component glue. The second test was successful with a rate of 10^{-7} mbar l/s. The corresponding parts will be replaced with an improved version where less welding is necessary. The system was installed and tested with several lowering cycles which also lead to a detailed procedure on how to operate it in manual mode. The manual operation uses a Teflon ring at the nonius as a break. However, the friction of this ring was not uniform and ranges with some slack were found, leading to an inaccurate positioning of the source with a position error of 1.7 cm. As an improvement of the lowering system, a motor was installed in September 2010. The corresponding controller counts the turns of the motor with much higher accuracy leading to a position error of 0.5 cm. This error is limited by systematics since the controller still counts turns and the corresponding change in position depends on the absolute position of the source. As a further improvement it is planned to use the perforation of the stainless steel band together with two ore more laser diodes to measure the movement of the metal band. With such a system an error of less than 0.1 cm can be reached. Furthermore, a remote control is under construction.

To protect the personnel working in the clean room from the radiation of the source, an additional shield is necessary. The construction of this shield, which will use 4 cm of Densimet (a tungsten alloy with high density which is not as brittle as pure tungsten and easy to machine) is ongoing.

At the end of September, the stainless steel band holding the source and its Ta holder has suffered a rupture during a calibration procedure. This lead to the holder and source being lost at the bottom of the cryostat. The cause of this rupture is under investigation but it is likely related to the operation of the motor, namely to the fact that the handling of the source parking position had not been implemented and that no proper protection against wrong operation was available.

At the time of writing we are building a new source holder (as a few sources are already available, see Section 10.1) and we will be starting to design and test a new source lowering system. Since it is difficult and costly to extract the source and the attached holder from the bottom of the liquid argon cryostat, we are investigating its impact on the

background given its current position. We are assuming 3 m of liquid argon between source and detectors and no shielding by the holder. The ^{228}Th source has a current activity of 30 kBq and a measured neutron flux of 1.3×10^{-3} n/(s·kBq). We obtain a background rate of 1-2·10^{-3} cnt/(kg·y·keV) and 5·10^{-5} cnt/(kg·y·keV) from gammas and neutrons, respectively, which is acceptable for GERDA Phase I.

10.3 Calibration Analysis Pipeline

In the search for the neutrinoless double beta of ^{76}Ge, a stable performance of the enriched diodes together with the readout electronic chain over long time periods as well as a good energy resolution are mandatory, since the sensitivity on the half life scales with $T_{1/2}^{0\nu\beta\beta} \propto \sqrt{1/\Delta E}$, where ΔE is the energy resolution at the Q-value of the decay (2039 keV). To ensure a stable performance, it is thus necessary to perform calibrations of the diodes throughout the entire data taking period.

Weekly calibrations of the diodes will be performed with a ^{228}Th source which is mounted permanently in the experimental setup. These calibration runs provide the energy calibrations of the detectors and can be used to monitor the performance stability of the single diodes in energy calibration and energy resolution. A continuous monitoring of the energy calibration of the single diodes is necessary to account for slight variations in the diodes performance with time when combining the data from several diodes in search for the neutrinoless double beta decay. The monitoring of specific lines can be used to identify periods in time for which single channels showed a degraded performance such that these time periods can be neglected in the final analysis.

Several energy reconstruction algorithms are used to obtain the raw energy estimator from the recorded waveforms of the diodes. The different reconstruction algorithms allow to study the systematic uncertainty in the final result on $T_{1/2}^{0\nu\beta\beta}$ of the ^{76}Ge isotope. One of the algorithms directly runs on the VME CPU of the FADCs such that it is available directly after the calibration and can thus be used for a blinding of the region of interest around the Q-value of the decay. However, the blinding procedure is also in need for an initial calibration of the VME energy estimator to identify single events which may end up in a region of interests with a predefined width ($\sim$10 keV) around the Q-value.

Thus it is necessary to have quick and reproducible calibrations of the energy scale of the single diodes. An iterative automated calibration routine has been developed to perform the calibration for the three different reconstruction algorithms. The routine starts from the full absorption peak (2614.5 keV) to have a rough initial calibration of the energy scale, and afterwards searches for additional lines in this freshly calibrated spectrum. This process is repeated iteratively several times to improve the energy calibration over a broader energy range. In addition to the energy calibration, the routine determines the energy resolution as a function of energy, in order to give an estimate of the energy resolution at the Q-value. For stability monitoring of the energy calibration and energy resolution the position and resolution of four spectral lines (at 583.2 keV, 1620.5 keV, 2103.5 keV and 2614.5 keV) are stored for each calibration run, each detector and each energy reconstruction algorithm. For every calibration, plots of the calibrated spectrum, the calibration and energy resolution

functions as well the monitoring lines are available via an online display. The online display also has links to the calibration parameters for each diode which can be used for analyses of the data taken after the specific calibration run.

Figure 19 shows a ^{228}Th spectrum for one of the natural Ge diodes being currently operated in GERDA, along with the results of a Monte Carlo simulation.
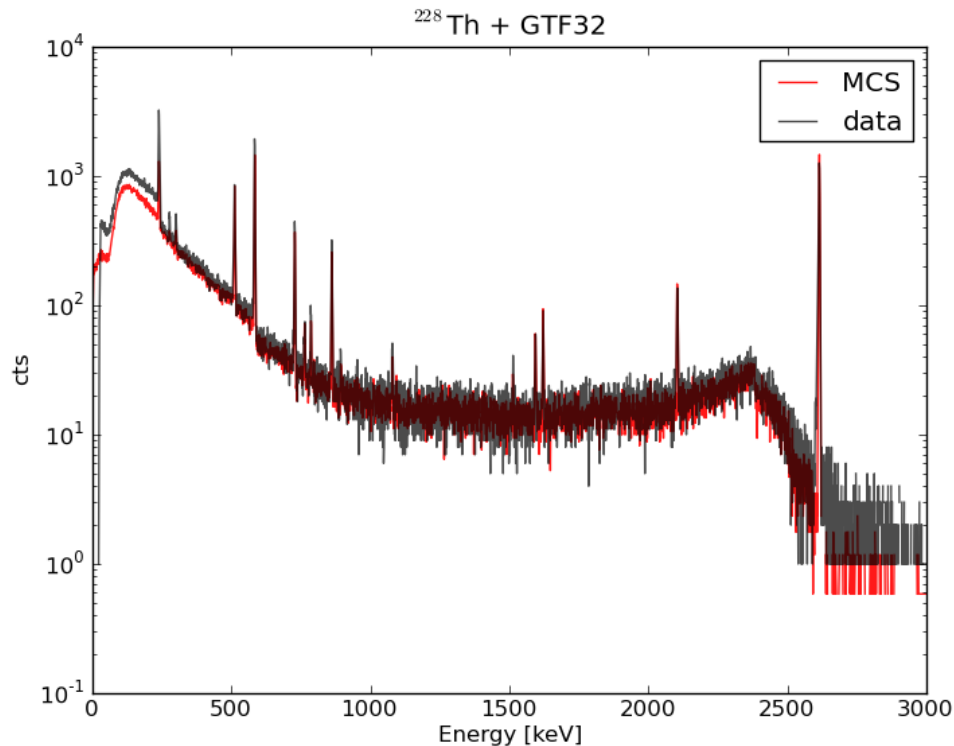

Figure 19: ^{228}Th spectrum for one of the natural Ge diodes currently operated in GERDA (grey), along with the results of a Monte Carlo simulation (red).

A general-purpose MySQL relational database has been developed in order to merge the information needed for analysis and monitoring of the stability and the response of each individual diode, including the calibration parameters described above. The database contains both static and dynamic information. The static part records the information that is not directly related to a given experimental run and contains data concerning the detectors, the experimental setup and the hardware. The dynamic part is storing the data closely related to the detector operation and data taking. An outline of the database design is presented in Fig. 20; it contains the following parameter:

- properties of each crystal
- installation and deinstallation history of each crystal
- acquired data sets

- data processing
- DAQ and electronics configurations
- calibration parameters
- calibration analysis history
- data quality check parameters

The basic structure of the database has been defined and the currently available information is filled. A web based interface for easy storing and retrieving information from the database is under construction.
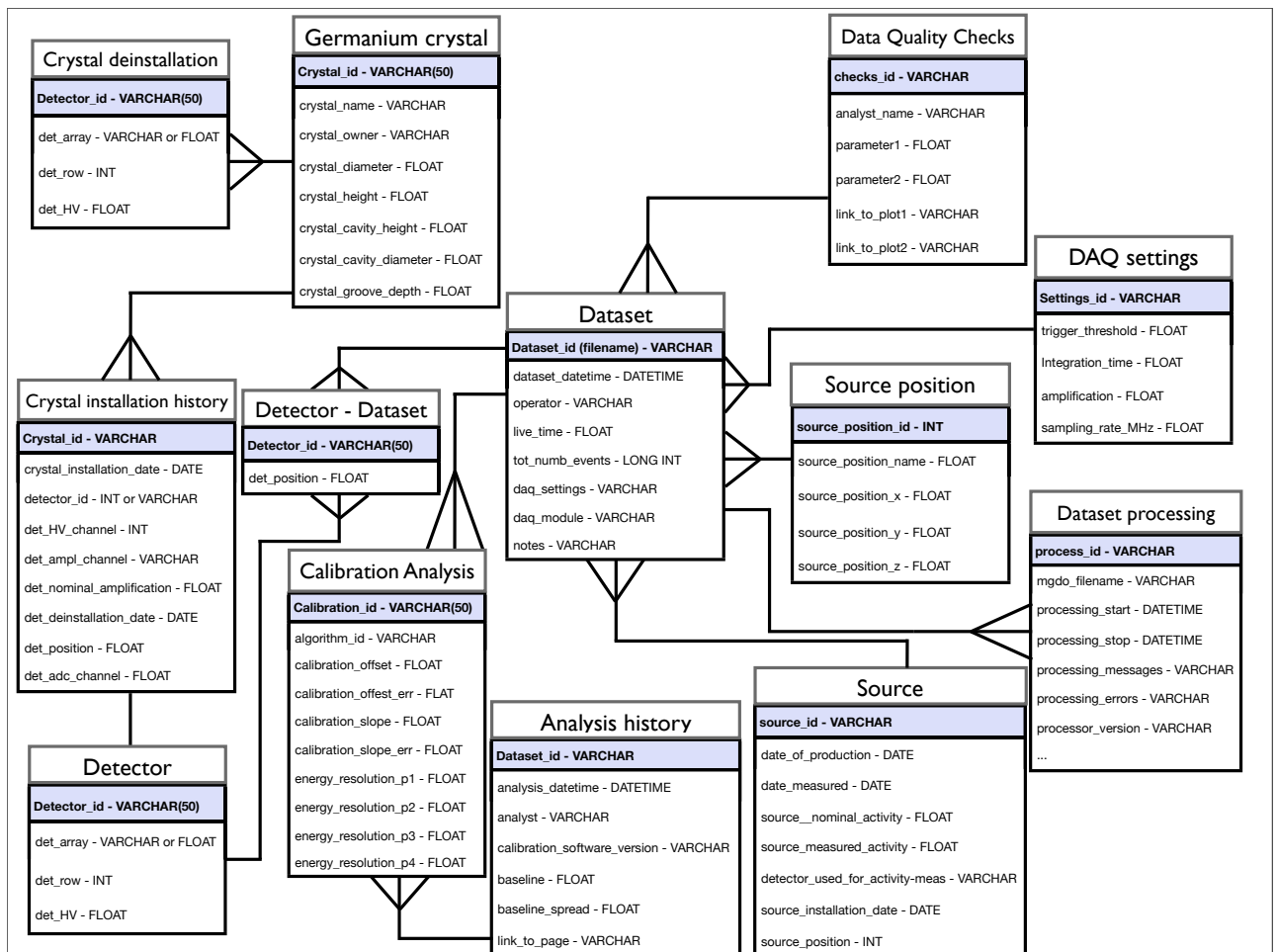

Figure 20: An outline of the MySQL database.

11 Data management and quality control

A new task group has been created to organize the data management and data quality control. Many pieces of hardware and software have been created or established already by the experts (see sect. 8). However, the coordination and control should ensure the most complete measurement and documentation of parameters for an efficient analysis. The handling of slow control and calibration is included in this work; data security is an essential issue. The online monitoring of the data, e.g., will set immediate alarms in case of unforeseen changes of any parameter.

The proposed data stream is sketched in Fig. 21. The interrelation between the hard-
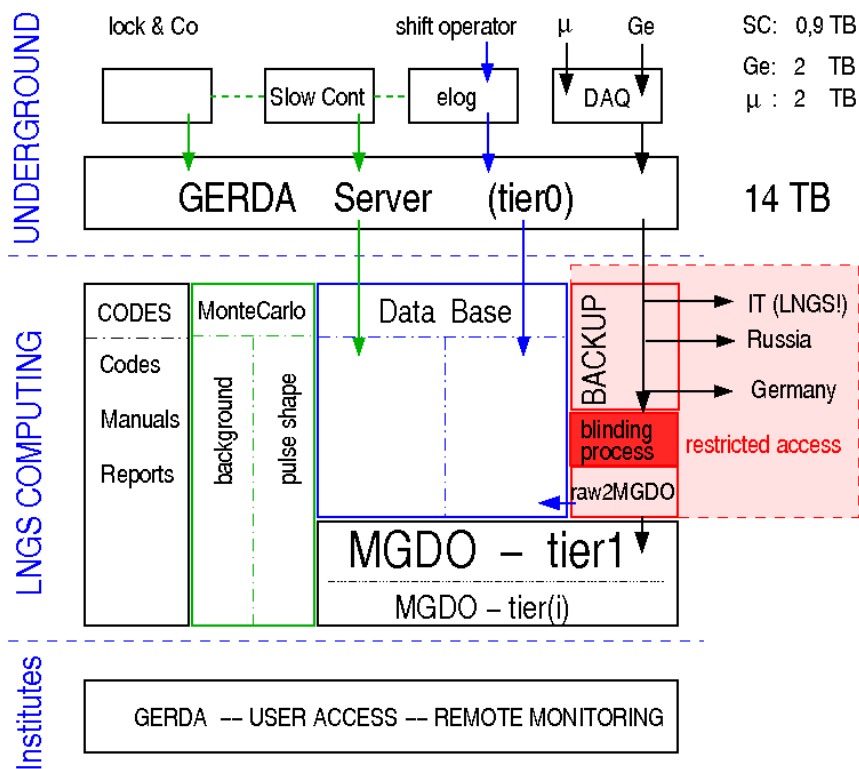

Figure 21: General scheme of data flow for storage, backup and analysis.

ware on the acquisition side and the storage side are shown, as well as the interconnection between data and simulation. The hardware part for the underground site close to the experiment is installed. A RAID array has been delivered. Script are tested with the present data from the background measurements, as well with other data e.g. from LArGe.

References

[1] M. Barnabe-Heider et al. JINST (in print)

[2] D. Budjas et al. JINST 4:P10007,2009

[3] I. Abt et al. Nucl.Instrum.Meth. A 577 (2007) 574

[4] M. Knapp, PhD thesis 2009, Eberhard Karls Universität Tübingen

[5] K. Freund, F. Ritter, B.Shaybonov and P. Grabmayr, GSTR-10-003, "Update on the Muon Veto – installation of the DAQ", Sep 2010

[6] M. Ballintijin, C. Loizides and C. Reed, Tree Analysis Modules, http://www.cmsaf.mit.edu/twiki/bin/view/Software/TAM

[7] V.D. Ashitkov *et al.*, [arXiv:nucl-ex/0309001].